International Journal of Surgical Pathology
1–11

DOI: 10.1177/10668969241246473
journals.sagepub.com/home/ijs
Sage

Periosteal Ewing Sarcoma with Distant Metastases: Report of Two Patients and Review of the Literature

Eva M. Pena-Burgos, MD[1], María C. Díez-Corral, MD[1], Eduardo J. Ortiz-Cruz, MD, PhD[2], Daniel Bernabéu, MD, PhD[3], Mar Tapia-Viñe, MD[3], Andrés Redondo, MD, PhD[4], Antonio Pérez-Martínez, MD, PhD[5], Alberto Peláez, MD, PhD[6], Clara Venegas Mascaró, MD[7,8], Adela Escudero López, MD, PhD[7,8], and Jose J. Pozo-Kreilinger, MD, PhD[9]

Abstract

Periosteal Ewing sarcoma (ES) is an exceedingly rare topographic subtype of the ES. To our knowledge, only 60 patients have been reported in the medical English language literature. It predominantly affects men in the second decade of life and arises in the long tubular bone diaphysis. PES rarely develops distant metastases. We report two patients of this rare ES location that were found on the distal tibial shaft and proximal femoral diaphysis of a 21-year-old man and an 8-year-old boy, respectively. Both patients were treated with neoadjuvant chemotherapy, wide resection, and adjuvant chemotherapy. One of our patients had lung metastases at the time of diagnosis and died 5 years later. The other patient presented intramedullary humeral bone metastasis 19 years after diagnosis. There has been no evidence of disease in the 26 years of follow-up. Close follow-up of periosteal ES is recommended because distant metastases may exceptionally occur, even several years after diagnosis.

Keywords

periosteal Ewing sarcoma, Ewing sarcoma, Ewing metastases, bone sarcoma

Introduction

In the last World Health Organization classification, the term Ewing sarcoma (ES) encompasses small round cell sarcomas showing fusion genes involving the *FET* family of genes and the *ETS* family of transcription factors.[1] New small round cell sarcomas with similar morphology than ES that present EWSR1-non-ETS fusions, *CIC* or *BCOR* rearrangements have been recently described and are considered to be distinct from ES.[1] Molecular confirmation tests are needed for an ES diagnosis. This type of sarcoma is treated with neoadjuvant chemotherapy that is based on the IE-VAC scheme (etoposide, ifosfamide, vincristine, doxorubicin, and cyclophosphamide) and/or radiotherapy, surgery, and adjuvant chemotherapy and/or radiotherapy.[1]

ES is the second most common primary malignant bone tumor in children and young adults.[1] It usually arises in the medullary cavity of the diaphysis or diaphyseal-metaphyseal region of long bones, the pelvis, and the ribs.[1] A total of 10% of all patients have been located in extraskeletal locations.[1] To our knowledge, only 60 periosteal ES have been reported in the medical literature.[2–18] The objective of this article is to present the clinical, radiological, and histopathological features of periosteal ES, as well as outline

[1]Pathology Department, Príncipe de Asturias University Hospital, Alcalá de Henares, Spain
[2]Orthopaedics and Traumatology Department, La Paz University Hospital, Madrid, Spain
[3]Radiology Department, La Paz University Hospital, Madrid, Spain
[4]Oncology Department, La Paz University Hospital, Madrid, Spain
[5]Pediatric Oncology Department, La Paz University Hospital, Madrid, Spain
[6]Molecular Pathology and Therapeutic Targets Group, La Paz University Hospital (IdiPAZ), Madrid, Spain
[7]Institute of Medical and Molecular Genetics (INGEMM), Hospital La Paz Institute for Health Research - IdiPAZ, Madrid, Spain
[8]Translational Research in Pediatric Oncology Hematopoietic Transplantation & Cell Therapy, Hospital La Paz Institute for Health Research - IdiPAZ, Madrid, Spain
[9]Patology Department, La Paz University Hospital, Madrid, Spain

Corresponding Author:
Eva M. Pena-Burgos, Department of Pathology, Hospital Universitario Príncipe de Asturias, Av. Principal de la Universidad, s/n, 28805, Alcalá de Henares, Madrid.
Email: evapenaburgos.ep@gmail.com

the management of two patients that presented this very rare location of ES.

Materials and Methods

La Paz University Hospital in Madrid is a tertiary hospital and one of the expert hospitals for bone and soft tissue tumor management in Spain. All the ES patients diagnosed in the Pathology Department at the La Paz University Hospital in Madrid between 1966 and 2022 were reviewed in the present study. Clinical information and radiological images were obtained from the medical records. All available materials from the pathology files were reviewed, including hematoxylin and eosin-stained slides, immunohistochemical stains, and molecular tests. Molecular testing in selected ES patients was completed retrospectively by next-generation sequencing (NGS) which allowed us to efficiently detect major genetic alterations, including fusion genes. DNA samples were analyzed using the customized panel mut4Child where 324 genes related to pediatric non-central nervous system tumors were sequenced by the Illumina platform (NovaSeq6000). Thereafter, raw data was analyzed by a tailor-made pipeline. DNA sequence reads were aligned on the human reference sequence hg19 using Burrows-Wheeler Aligner (v0.7.17). polymerase chain reaction (PCR) duplicates were removed by Picard (v2.18.25), and recalibration of the reads was done by the Genome Analysis Toolkit (GATK v4.1.4.9). Fusion genes were studied using Manta software (v1.6.0) and annotated in a Variant Call File) with the gene name of, at least, one partner, structural variant type, genomic position, and number of pair and split-read alignments. Fusion genes were filtered and identified using VarSeq™ v2.5.0 and the Integrative Genomics Viewer.

Results

Three hundred and nine patients of ES patients were registered. Only two of them (0.64%) had a periosteal location. Consent for publication was obtained from the patient and/or families.

Patient 1

A previously healthy 21-year-old man was referred to our center because of pain and swelling in his right tibia after a local trauma. He had been noticing a mass in the area for 3 years. A physical examination revealed a painful mass on the internal surface of his tibial distal diaphysis.

The radiograph showed an irregular destructive pattern on the surface of the medial cortex of the tibial shaft, with

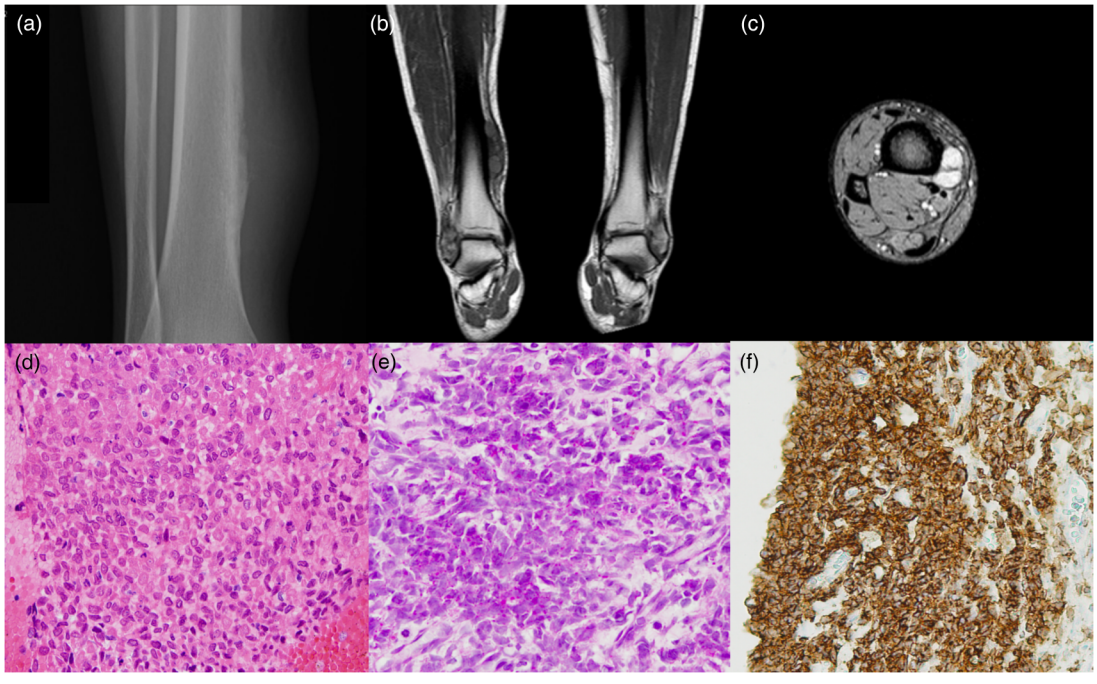

Figure 1. (a) Initial plain radiography: Internal distal diaphyseal periosteal tibial irregularity, with no cortical nor medullary distortion. (b) Initial T1-WI MRI: Hypointense mass closely adherent to the periosteum. (c) Initial T2-WI MRI: Hyperintense lobulated mass. (d) H&E, x100: Small to medium size round blue cells with a diffuse growth pattern. (e) PAS, x200: PAS cytoplasmic positivity and irregular nuclei without nucleoli. (f) CD99, x200: Diffuse membranous positivity. MRI, magnetic resonance imaging; WI, weighted image; PAS, periodic acid-Schiff.

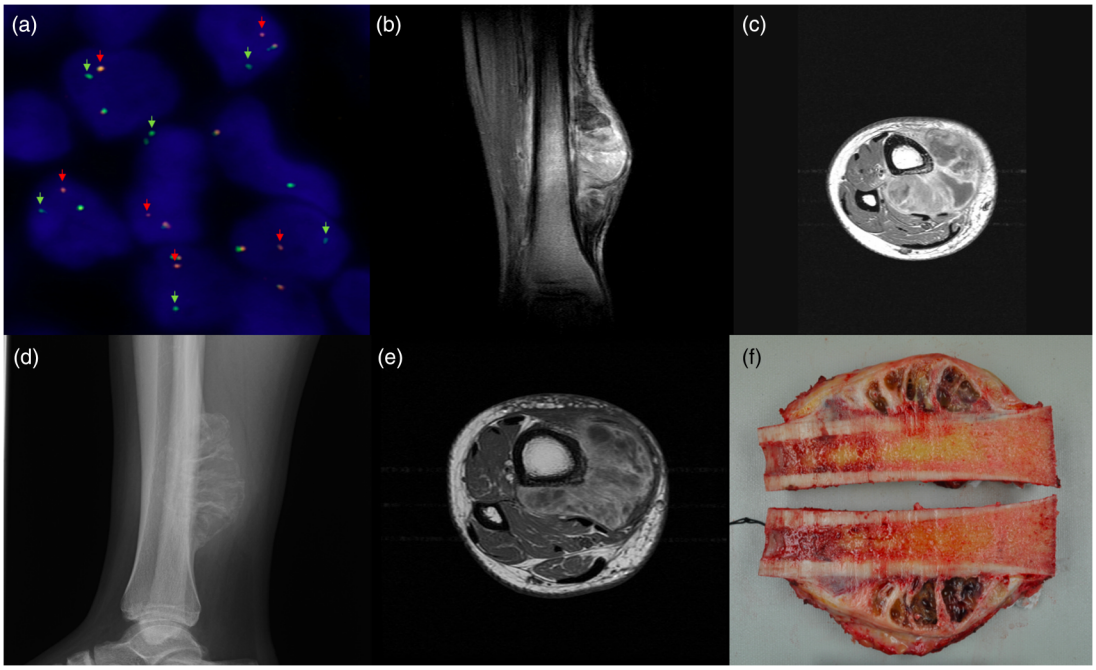

Figure 2. (a) FISH: *EWSR1* gene rearrangement. (b) Pre-chemotherapy sagittal T1-FatSat-CE-WI MRI: Heterogeneous enhancement of the mass with cortical involvement and medullar edema pattern enhancement. (c) Pre-chemotherapy axial T1-CE-WI MRI: Heterogeneous enhancement of the mass and cortex with cystic necrotic areas. (d) Post-chemotherapy plain radiography: Egg-shell calcified mass with septa from periosteal uplift in the distal tibial shaft. (e) Post-chemotherapy CE-MRI: Decreased size of the mass with increased areas of necrosis. (f) Macroscopic examination: Internal tibial periosteal mass with cavities separated by osseous walls. MRI, magnetic resonance imaging; WI, weighted image.

some periosteal reaction, and an associated soft tissue mass. Neither the deep zone of the cortex nor the medullary cavity seemed to be affected (Figure 1a). Magnetic resonance imaging (MRI) revealed a 5×2 cm lobulated mass closely adherent to the periosteum, which was isointense to muscle on T1-weighted image (WI) (Figure 1b), clearly hyperintense on T2*-WI (Figure 1c) and showed no surrounding inflammatory changes. After gadolinium administration, a mostly peripheral enhancement was seen. The first tentative diagnosis was a post-traumatic subperiosteal hematoma, with a malignant tumor having been less probable. The CT extension study showed a less than 1 cm nodular lesion in the inferior right lobe and small adenopathies in the axillar and inguinal region. A bone scintigraphy revealed uptake only in the right tibial region.

An ultrasound-guided core biopsy of the mass was performed. The histopathological analysis showed small to medium size uniform round blue cells with a diffuse growth pattern (Figure 1d). The cells presented indistinct cytoplasmic membranes, ill-defined scanty eosinophilic cytoplasm and irregular nuclei with stippled chromatin and inconspicuous nucleoli (Figure 1d and 1e). Periodic acid-Schiff staining revealed prominent cytoplasmic glycogen granules (Figure 1e). Some apoptotic cells were present. No rosettes nor gland formation were identified. In terms of immunohistochemistry, the tumor cells showed diffuse membranous positivity for CD99 (Clone 12E7, ready to use (RTU), Agilent-Dako) (Figure 1f) and a cytoplasmatic reaction to vimentin (Clone V9, RTU, Agilent-Dako). These cells were negative for keratin (Clone AE1/AE3, RTU, Agilent-Dako), CD45 (Clones 2B11 and PD7/26, RTU, Agilent-Dako), DNTT (Clone EP266, RTU, Agilent-Dako), S100 protein (Polyclonal, RTU, Agilent-Dako), muscle-specific actin (Clone HHF35, RTU, Agilent-Dako), MyoD1 (Clone 5.8A, RTU, Agilent-Dako), and synaptophysin (Clone DAK-SYNAP, RTU, Agilent-Dako). A molecular biology study for the translocation of the *EWSR1* gene using the FISH technique on interphase nuclei (Vysis LSI EWSR1 Break Apart FISH Probe Kit, Abbott) was positive in 77% of the nuclei (Figure 2a). Based on clinical, radiological, histopathological, and molecular findings, a diagnosis of periosteal ES was made.

The pre-chemotherapy MRI (Figure 2b and c) showed that the tumor had grown significantly to 9×5 cm maintained the T1-WI hyposignal, which had scattered areas of hyperintensity that were suggestive of hemorrhagic changes, and had a markedly heterogeneous T2-WI hypersignal with the presence of cystic areas of necrosis inside. The adjacent bony cortex showed complete infiltration in 3/5 of the tibial perimeter, with some areas of slight

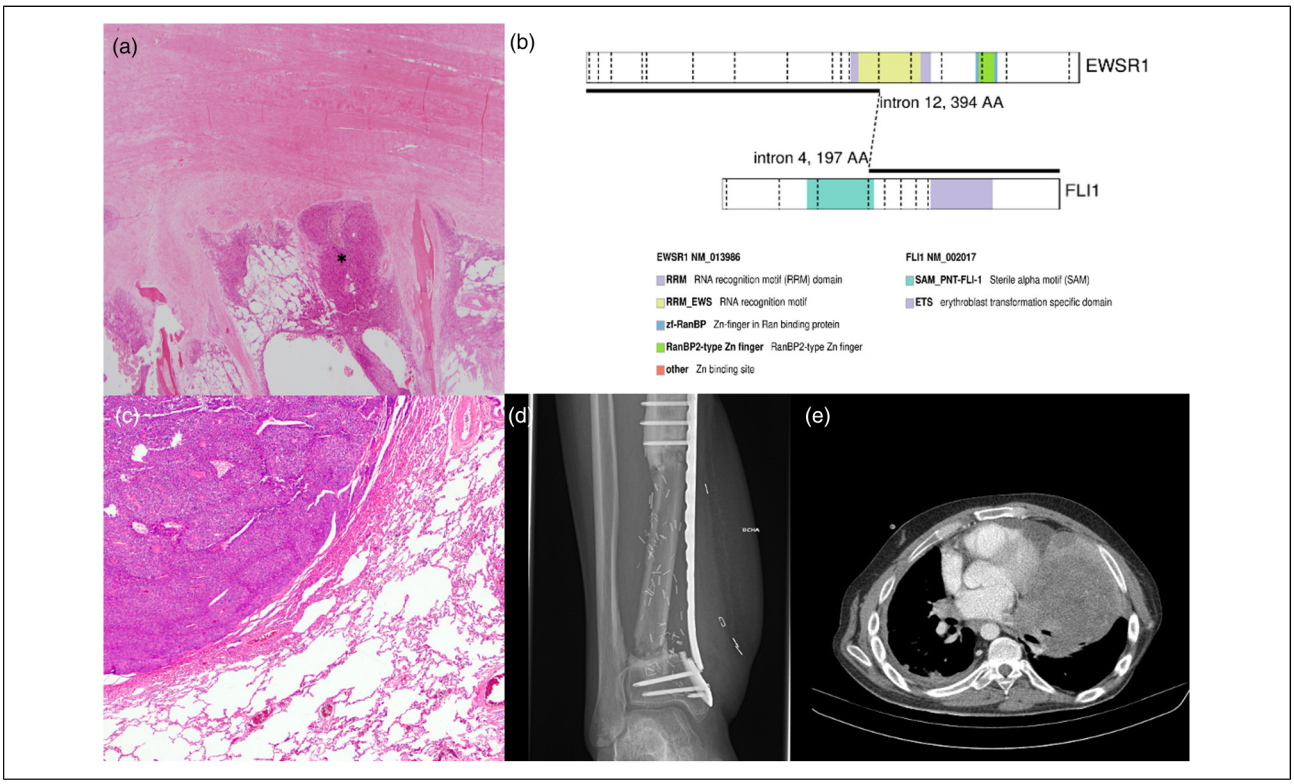

Figure 3. (a) H&E, x40: Post-chemotherapy changes with residual tumoral cells (*). (b) NGS: Schematic of the *EWSR1::FLI1* translocation involved. (c) H&E, x100: ES pulmonary metastasis. (d) Post-surgery plain radiography: Distal osteosynthesis material failure. (e) Chest CT: Pulmonary unresectable metastases. ES, Ewing sarcoma; NGS, next-generation sequencing.

periosteal reaction, and an edema pattern in the adjacent medullary cavity. After gadolinium administration, marked heterogeneous enhancement of the mass and areas of cortical infiltration were observed, as well as a diffuse enhancement in the adjacent medullary cavity and around the soft tissue mass. A bone marrow biopsy showed no evidence of infiltration. The patient started neoadjuvant chemotherapy with the IE-VAC scheme. After chemotherapy, radiographs showed marked calcification of the surface of the mass (from periosteal uplift) with internal septa (Figure 2d). MRI evidenced a slight decrease in the size of the mass with an increase in necrotic areas and markedly less heterogeneous enhancement after gadolinium (Figure 2e).

In the post-chemotherapy extension CT, several millimetric (6 mm the highest) nodular images were found in both lungs, as well as inguinal and iliac adenopathies. The patient underwent a limb salvage surgery. A wide intercalary diaphyseal-metaphyseal tumor resection of the distal tibia was performed. Bone reconstruction was done with a vascularized contralateral fibula autograft and osteosynthesis with a locking compression plate was performed. To give the best coverage to the bone reconstruction, a microvascular free tissue transfer with the latissimus dorsi flap was carried out.

Examination of the tibial resection was performed in the Pathology Department. It measured 14 cm long and included skin, soft tissues, and a bone segment of the diaphysis of the right tibia. A diaphyseal periosteal mass at the medial margin of the tibia mass composed of cavities filled with grayish gelatinous content separated by osseous strands was present (Figure 2f). An exhaustive sampling of the tumor was done, including those areas related to the cortical and the underneath medullary region. No cortical, medullary, or soft tissue infiltration were macroscopically detected. Post-chemotherapy changes (tumoral necrosis, fibrosis, and interstitial hyalinization) affected 85% of the tumoral cells (Figure 3a). The residual viable cells were identical to those of the previous core needle biopsy. Surgical margins were free.

No early post-operative complications arose. Post-operative chemotherapy was administered continuing the same regimen. A year after the bone surgery, an atypical segmentectomy of the medial right pulmonary lobe was performed. The diagnosis of ES metastases was made (Figure 3c). The retrospective analysis by NGS only detected *EWRS1::FLI* fusion gene (Figure 3b), the same genetic alteration previously identified in the original tumor. After the pulmonary nodule resection, chemotherapy with high-dose ifosfamide was initiated. Four years after the first bone surgery, the proximal fibular osteosynthesis developed pseudoarthrosis, and the distal osteosynthesis material was broken (Figure 3d); therefore, the

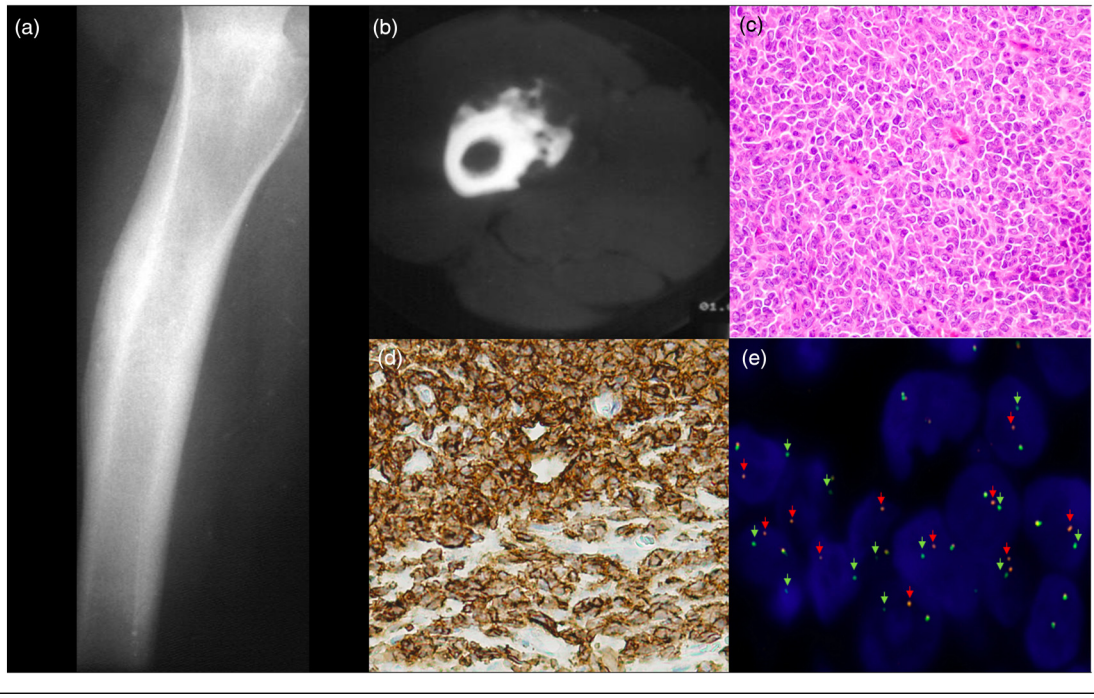

Figure 4. (a) Initial femoral plain radiography and (b) Initial CT: Thickening of the medial femoral shaft cortex, with irregular periosteal reaction and no medullary distortion. (c) H&E, x400: Small to medium size round blue cells with a diffuse growth pattern. (d) CD99, x200: Diffuse membranous positivity. (e) FISH: *EWSR1* gene rearrangement.

patient was operated on again with an iliac crest autograft and a new medial osteosynthesis plate. The pulmonary disease continued progressing, being unresectable (Figure 3e). The patient received several lines of systemic therapy, with one of them including a clinical trial by the Spanish Group of Sarcoma Research (GEIS), which assessed the efficacy and safety of nab-paclitaxel. The patient died 5 years after diagnosis.

Patient 2

A previously healthy 8-year-old boy was referred to our center because he presented swelling and pain in his left femur for a month. He did not refer to any prior local trauma. A physical examination detected a painful mass on the external surface of the medial femoral diaphysis.

The plain radiography (Figure 4a) and CT (Figure 4b) images showed cortical thickening with irregular periosteal reaction in the medial area of the proximal femoral shaft. No densitometric involvement of the bone marrow was detected. An ultrasound-guided core biopsy was performed. A small and round cell sarcoma similar to patient 1 was seen (Figure 4c and 4d). A molecular biology study for the translocation of the *EWSR1* gene using the FISH technique on interphase nuclei (SureFISH EWING 5' and 3' Chr22 probes, Agilent-Dako) was positive in 95% of the analyzed nuclei (Figure 4e). The extension study showed no other lesions. Based on the clinical, radiological, histopathological, and molecular findings, a diagnosis of periosteal ES was made.

A bone marrow biopsy showed no evidence of infiltration. The patient started neoadjuvant chemotherapy with the Pediatric Hemato-Oncology Spanish Society Protocol. No metastases were present in the post-chemotherapy extension study. The patient underwent a limb salvage surgery. A wide intercalary diaphyseal tumor resection of the femur was performed. The bone reconstruction was performed with an intercalary allograft and an osteosynthesis with an intramedullary rod and a distal locking compression plate was necessary.

An intercalary femoral resection was performed in the Pathology Department, which measured 21.5 cm and included soft tissues and the bone segment of the diaphysis of the left femur. An external femoral diaphyseal periosteal whitish thickening was observed, with partial cortical erosion and medullary sclerosis (Figure 5a). Post-chemotherapy tumoral necrosis affected 90% of the tumoral cells (Figure 5b). Small tumor foci were detected infiltrating the cortical bone surface (Figure 5c) but no medullary infiltration was demonstrated. An exhaustive sampling of the tumor similar as in the first case was done. Surgical margins were free. A second surgery was performed due to a deviation of the bone after a fall and a plate was added to the distal femur (Figure 5d). Post-operative chemotherapy was administered.

No evidence of disease was present 19 years after diagnosis until a left humerus pathological fracture was detected

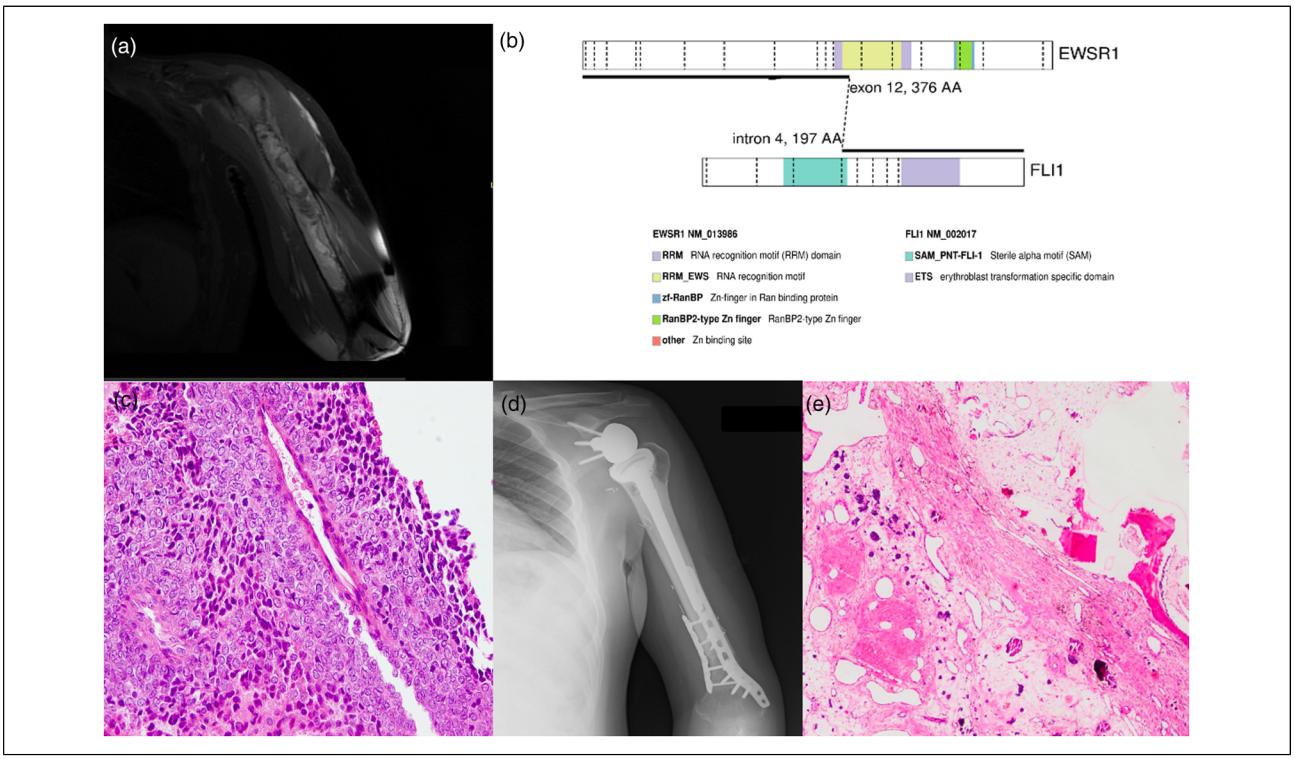

Figure 6. (a) Humeral pre-chemotherapy MRI: Infiltration of the medullary cavity of the proximal 2/3 of the humerus due to a solid tumor with hypersignal in T2-WI. (b) NGS: Schematic of the *EWSR1::FLI1* translocation involved. (c) H&E, x100: Small to medium size round blue cells. (d) Humeral post-surgery plain radiography: Composite allograft prosthesis with reversed humeral prosthesis (MUTARS®) and intercalary allograft. (e) H&E, x40: post-chemotherapy changes with residual tumoral cells. NGS, next-generation sequencing; MRI, magnetic resonance imaging; WI, weighted image.

by radiological images (Figures 5e and 6a). A tumoral lesion in the proximal epiphysis, metaphysis, and diaphysis was seen. A staging study did not detect other lesions. A percutaneous core biopsy was performed, with a densely packed small round cell tumor, histologically similar to his previous femoral biopsies. A diagnosis of metastatic ES was done (Figure 6c). The presence of *EWRS1::FLI* fusion gene (Figure 6b) and no other genetic mutations was retrospectively confirmed by NGS, being the same fusion gene as in the original tumor.

Neoadjuvant chemotherapy with the IE-VAC scheme was administered. The patient underwent an intraarticular wide proximal humeral resection. A composite bone reconstruction was necessary with a reversed humeral prosthesis (MUTARS®) (Figure 6d) and an intercalary allograft. An osteosynthesis with anteromedial and posterolateral locking compression plate plates was carried out. Examination of the proximal humeral resection was performed in the Pathology Department. Post-chemotherapy necrosis affected 95% of the tumoral cells (Figure 6e). Surgical margins were free. Adjuvant chemotherapy was administered with the EVAIA scheme. Seven years after the humeral metastasis, the patient is free of disease.

Discussion

Periosteal ES is an extraordinarily rare location for ES characterized by a tumoral epicenter in the subperiosteal area, which usually does not extend to the medullary cavity.[16] A thin layer of periosteum radiologically encases the tumor from the adjacent soft tissues.[17] Kumar et al[17] recently radiologically described some tumors in bones with a fine cortex that may present medullary involvement. To our knowledge, only 60 periosteal ES patients have been reported in the medical literature[2–9,11–18] (Table 1).

We report two new tumors in an 8-year-old man and a 21-year-old boy. Periosteal ES presents a marked men predominance (thirty-four men vs nine women) and predominantly occurs in the second decade of life. Only eight tumors have been found in patients over 20 years old.[3,5,7,10,15,17] Another two tumors in children younger than 10 have been described.[3] Periosteal ES more frequently arises in the diaphysis of long bones (19 tumors in the femur, 12 in the humerus, and five in the tibia), although other bones have been affected (two tumors in the ilium, two in the superior pubic ramus, and one in the scapula).[3,17]

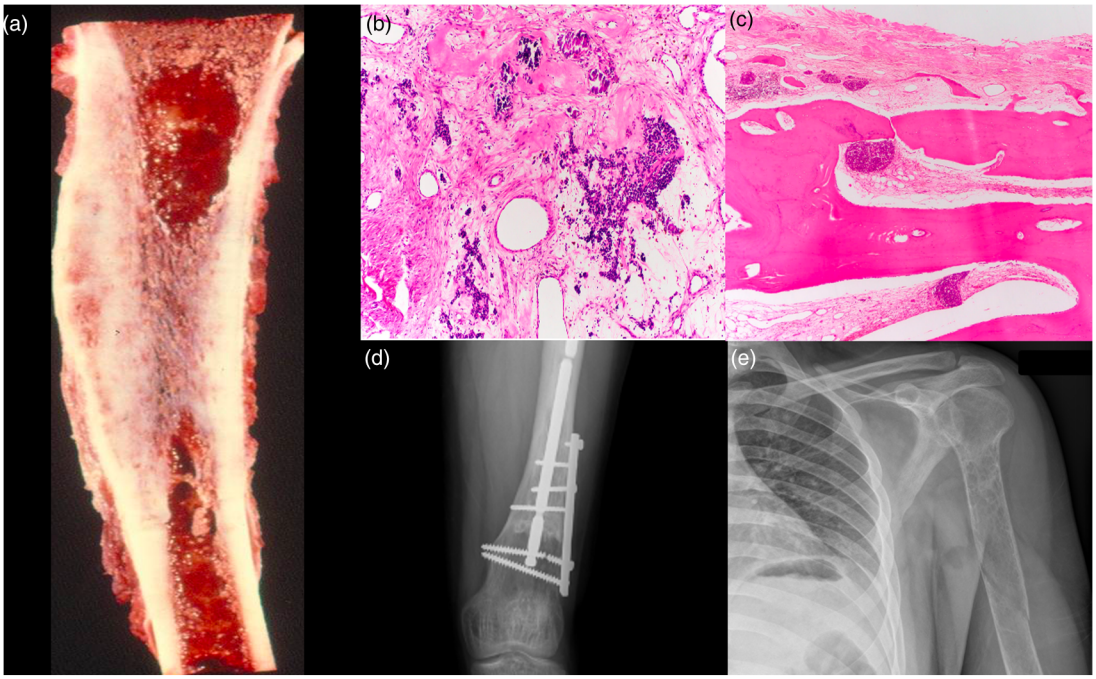

Figure 5. (a) Macroscopic examination: External femoral diaphyseal periosteal whitish thickening, partial cortical erosion, and medullary sclerosis. (b) H&E, x40: Post-chemotherapy changes with residual tumoral cells. (c) H&E, x100: Microscopic cortical infiltration (fx1). (D) Femoral post-operatory plain radiography: Intercalary diaphyseal resection, osteosynthesis, and plate. (e) Humeral plain radiography: Widening of the medullary cavity with lytic areas and pathological fracture.

Given the infrequency of this tumoral location, this type of sarcoma usually presents a low clinical-radiological suspicion. Periosteal ES is radiologically distinguished from medullary ES due to the absence of medullary and soft tissue invasion.[17] No Codman triangle is seen in periosteal ES.[16] Sometimes extraskeletal ES may mimic periosteal ES when it erodes the cortex and produces a periosteal reaction or causes surface bone erosion, but MRI and CT scans demonstrate the non-periosteal origin of extraskeletal ES.[17] In the Violon et al[16] series, 50% of the patients were misdiagnosed as soft tissue tumors. The radiological features of periosteal ES are similar to other periosteal malignant tumors (chondrosarcoma, osteosarcoma) except for the absence of a calcified matrix.[17] Periosteal ES may also be confused with benign entities such as a subperiosteal aneurysmal bone cyst that presents the characteristic fluid-fluid levels on MRI scans, or periosteal hemangioma, which has an eccentric growth from the periosteal uplift and cortical erosion.[17] Non-tumoral lesions such as subperiosteal hematoma, osteomyelitis, intracortical abscess, and stress fracture can also be included in the differential diagnosis.[18]

Periosteal ES are histopathologically and immunohistochemically similar to medullary ES and extraskeletal ES.[7] The main histological differential diagnosis of small round cell tumors should be made with CIC rearranged sarcomas, BCOR rearranged sarcomas, round cell sarcoma with EWSR1-non-ETS fusion, desmoplastic small round cell tumor, alveolar rhabdomyosarcomas, small cell osteosarcomas, mesenchymal chondrosarcomas, lymphomas, and neuroblastomas.[17] CIC rearranged sarcomas may be CD99 focal positive but are WT1 and ETV4 positive and often present the CIC::DUX4 fusion gene. A round to spindle cell morphology, variable myxoid stroma, CyclinD1, SATB2 and BCOR immunostaining and BCOR genetic alterations are seen in BCOR rearranged sarcomas. Round cell sarcoma with *EWSR1::PATZ1* fusion genes express neurogenic and myogenic markers, present a fibrous stroma, and FISH technique may not detect the fusion gene so other molecular test are needed to determine the genetic alteration of these tumors. Round cell sarcoma with *EWSR1::NFATC2* fusion gene are round or fusocelular CD99 positive cells in a myxohyaline stroma and molecular studies are fundamental to differentiate it from ES. Desmoplastic small round cell tumor is composed by CD99 negative, and C-terminus WT1, keratin and desmin strong immunoreactive cells in a desmoplastic stroma. Alveolar rhabdomyosarcomas are soft tissue tumors that display strong and diffuse myogenin stain and *FOXO1* rearrangement. Some small cell osteosarcomas may show CD99 positive staining, but they contain osteoid matrix and SATB2 positivity. Mesenchymal chondrosarcomas may also show CD99 positive staining, but areas of a chondroid matrix with non-atypical chondrocytes, which display

Table 1. Previous Periosteal ES Reported Patients in Literature.

Case	Article, year	Age, sex	Site	Treatment	Molecular findings	Follow-up
1	Bator, 1986	13, M	Humerus, diaphysis	NA CT + radical resection + A CT	Not mentioned	2 years, NED
2	Kolar, 1989	13, M	Femur, diaphysis	NA CT and RT + resection	Not mentioned	1.5 years, NED
3	Kolar, 1989	8, M	Femur, diaphysis	NA CT and RT + extirpation	Not mentioned	1 year, metastasis in humeral condyle and local recurrence treated with RT; 3.5 years, NED
4	Kolar, 1989	16, M	Tibia, diaphysis	NA CT and RT + resection	Not mentioned	1.5 years, NED
5	Kolar, 1989	15, M	Femur, diaphysis	NA CT and RT + resection	Not mentioned	2.5 years, NED
6	Kolar, 1989	36, M	Femur, diaphysis	NA CT and RT + resection	Not mentioned	1.5 years, NED
7	Kolar, 1989	3.5, M	Scapula, muscular invasion	NA CT and RT + resection	Not mentioned	1 year, dead
8	Wuisman, 1992	18, M	Humerus, diaphysis	Wide resection	Not mentioned	INA
9	Wuisman, 1992	11, F	Humerus, diaphysis	Wide resection	Not mentioned	INA
10	Wuisman, 1992	15, M	Femur, diaphysis	NA CT and RT + wide excision	Not mentioned	INA
11	Shapeero, 1994	11, F	Humerus, diaphysis	NA CT and RT + radial excision + A CT and RT	Not mentioned	2 years, NED
12	Shapeero, 1994	13, M	Humerus, diaphysis	NA CT + wide excision + A CT	Not mentioned	2 months, NED
13	Shapeero, 1994	13, M	Humerus, diaphysis	wide excision + A CT	Not mentioned	8 years, NED
14	Shapeero, 1994	14, M	Femur, distal metadiaphysis	NA CT + wide excision + A CT	Not mentioned	6 years, NED
15	Shapeero, 1994	14, M	Femur, diaphysis	NA CT and RT + wide excision	Not mentioned	6 years, radio-induced osteosarcoma, amputation; 10 years, NED
16	Shapeero, 1994	14, F	Humerus, diaphysis	NA CT + wide excision + A CT	Not mentioned	1.5 years, NED
17	Shapeero, 1994	15, M	Femur, diaphysis	NA CT and RT + wide excision + A CT	Not mentioned	2 years, NED
18	Shapeero, 1994	15, M	Femur, diaphysis	NA CT + wide excision	Not mentioned	6 years, NED
19	Shapeero, 1994	16, M	Fibula, distal metadiaphysis	NA CT and RT + wide excision + A CT and RT	Not mentioned	5 years, NED
20	Shapeero, 1994	18, M	Humerus, diaphysis	NA CT + wide excision + A CT	Not mentioned	2.5 years, NED
21	Shapeero, 1994	30, M	Humerus, diaphysis	NA CT + wide excision + A CT	Not mentioned	2.5 years, NED
22	Kenan, 1994	13, M	Tibia, diaphysis	NA CT + wide resection	Not mentioned	3 years, NED
23	Declerck, 1995	INA	INA	INA	Not mentioned	INA
24	Kollender, 1999	16, M	Femur, diaphysis	NA CT + wide resection + A CT	Not mentioned	3 years, NED
25	Kollender, 1999	27, M	Femur, diaphysis	NA CT and RT + wide resection + A CT and RT	Not mentioned	1.5 years, NED
26	Hatori, 2001	20, F	Humerus, distal third	NA CT and RT + wide excision + A CT	Not mentioned	6 years, NED
27	Hatori, 2001	15, F	Humerus, distal metaphysis	Wide excision	Not mentioned	8 years, NED

(continued)

Table 1. (continued)

Case	Article, year	Age, sex	Site	Treatment	Molecular findings	Follow-up
28	Hatori, 2001	16, F	Femur, diaphysis	Wide excision	Not mentioned	4 years, NED
29	Delepine, 2002	14, M	Femur, diaphysis	NA CT + en bloc resection + A CT	Not mentioned	13.5 years, NED
30	Delepine, 2002	12, M	Femur, diaphysis	NA CT + resection + A CT	Not mentioned	13 years, NED
31	Delepine, 2002	18, M	Femur, diaphysis	NA CT + partial cortical excision + A CT	Not mentioned	2 years, NED
32	Delepine, 2002	17, M	Femur, diaphysis	NA CT + total diaphysis resection	Not mentioned	1,5 years, NED
33	Erlemann, 2002	28, M	Humerus, diaphysis	NA CT + wide resection + A CT	Not mentioned	NED
34	Yoshida, 2005	6, M	Humerus, proximal epimetaphysis	NA CT + Marginal or intralesional resection and RT + A CT	No fusions detected (RT-PCR)	1 year, NED
35	Aymoré, 2005	12, M	Femur	NA CT + cortical segmental resection	Not mentioned	2 years, NED
36	Hakozaki, 2007	13, M	Femur, diaphysis	NA CT + wide excision + A CT	EWS-FLI1 type 1 chimeric fusion (RT -PCR)	1.5 years, NED
37	Bonvin, 2007	INA	INA	INA	INA	INA
38	Bedard, 2017	65, M	Tibia, proximal diaphysis	Neoadjuvant chemotherapy, radical resection, and adjuvant chemotherapy	EWSR1 gene rearrangement (FISH)	INA
39	Violon, 2022	INA	Long bone, diaphysis	INA	Not mentioned	INA
49	Violon, 2022	INA	Long bone, diaphysis	INA	Not mentioned	INA
50	Violon, 2022	INA	Long bone, diaphysis	INA	Not mentioned	INA
51	Violon, 2022	INA	Long bone, diaphysis	INA	Not mentioned	INA
52	Violon, 2022	INA	Long bone, diaphysis	INA	Not mentioned	INA
53	Violon, 2022	INA	Long bone, diaphysis	INA	Not mentioned	INA
54	Kumar, 2022	21, M	Femur, diaphysis	NA CT + Radical resection with hemicortical femur resection and allograft reconstruction	Not mentioned	9 years, NED
55	Kumar, 2022	11, F	Tibia, diaphysis	NA CT + Radical resection with intercalary allograft reconstruction	Not mentioned	11 years, NED
56	Kumar, 2022	20, M	Superior pubic ramus	NA CT + hemipelvectomy and radical resection	Not mentioned	10 years, NED
57	Kumar, 2022	12, F	Ilium	NA CT + hemipelvectomy	Not mentioned	1.5 years, lung metastasis treated with RT, dead
58	Kumar, 2022	41, M	Tibia, diaphysis	CT and RT	Not mentioned	9 years, NED
59	Kumar, 2022	21, M	Ilium	NA CT + hemipelvectomy, partial sacrectomy and S1, S2 and S3 laminectomy	Not mentioned	8 months, lung and brain metastases treated with RT, dead
60	Kumar, 2022	66, F	Superior pubic ramus	NA CT and RT + radical resection	Not mentioned	7 years, NED
61	Patient 1, present study, 2024	21, M	Tibia, distal diaphysis	NA CT + intercalary diaphyseal-metaphyseal resection	EWSR1 gene rearrangement (FISH)	1 year, lung metastasis treated with surgery and CT; 5 years, dead

(continued)

Table 1. (continued)

Case	Article, year	Age, sex	Site	Treatment	Molecular findings	Follow-up
				and fibula allograft reconstruction + A CT	*EWRS1::FLI* fusion genes (NGS)	
62	Patient 2, present study, 2024	8, M	Femur, diaphysis	NA CT + wide resection and allograft reconstruction + A CT	EWSR1 gene rearrangement (FISH) *EWRS1::FLI* fusion genes (NGS)	19 years, humeral metastasis treated with surgery and A + NA CT; 26 years, NED

ES, Ewing sarcoma; NA, neoadjuvant; A, adjuvant; CT, chemotherapy; RT, radiotherapy; NED, no evidence of disease; INA, information not available; RT-PCR, reverse transcription-polymerase chain reaction; FISH, fluorescent in situ hybridization; NGS, next-generation sequencing.

immunoreaction against SOX9 and *HEY1::NCOA2* fusion genes, are found. Lymphomas demonstrate CD45 positivity and neuroblastomas are positive against chromogranin and synaptophysin, and are CD99 negative.[2]

Molecular studies of periosteal ES were mentioned only in three previous articles. Hakozaki et al reported a periosteal ES tumor with a *EWS::FLI1* fusion that was detected by a reverse transcription-polymerase chain reaction (RT-PCR)[13] while Yoshida et al did not find neither a *EWS::FLI1* or a *EWS::ERG* fusion gene by RT-PCR, and proposed that other gene fusions might be related to periosteal ES.[11] In both our tumors, the *EWSR1* gene rearrangement was detected using the FISH technique and recently the *EWRS1::FLI* fusion gene was detected in the NGS.

All ES are managed with the same treatment protocol. Patients start with systemic neoadjuvant chemotherapy and/or radiotherapy for micrometastases eradication,[19] continue with surgical resection for local control, and conclude with adjuvant chemotherapy and/or radiotherapy. The appearance of osteosarcoma following radiotherapeutic treatment has been reported in one patient.[5] Periosteal ES usually lacks metastases, although the mean follow-up in previously reported tumors is only 3.1 years. This may be due to the anatomical barriers surrounding the origin (cortical bone and periosteum).[13] Only three previously reported tumors developed distant metastasis in the humeral bone,[3] in a lung,[17] and in the brain,[17] which were detected within the first 1.5 years after the diagnosis. In one of our patients, lung metastasis was detected at the time of diagnosis. In the other patient, bone metastasis was detected nineteen years after the initial diagnosis. Remote ES metastasis (> 5 years from the primary tumor) have not yet been described in periosteal ES. In our patient 2, it may be related to anatomical barriers surrounding the tumor and the small percentage (5%) of viable tumoral cells after initial chemotherapy.

Conclusion

Periosteal ES is an extremely rare tumoral location with histological, immunohistochemical, and molecular features that allow for an accurate diagnosis. Periosteal ES should be considered in clinical and radiological differential diagnoses of juxtacortical bone tumors. A precise diagnosis is needed for the sarcoma to not be misdiagnosed as a benign lesion and also in order to perform the correct initial management strategies. Carrying out a close follow-up is recommended as the possibility of there being metastasis exists despite its low reported frequency, even several years after diagnosis.

Authors Contributions

Conception and design of the study and acquisition and analysis of data: Pena-Burgos EM, Ortiz-Cruz EJ, and Pozo-Kreilinger JJ. Radiology images: Bernabéu D, Tapia-Viñe M. Pathology figures: Pena-Burgos EM, Díez Corral MC, and Pozo-Kreilinger JJ. Molecular studies: Peláez A, Venegas Mascaró C, and Escudero López A. Drafting the manuscript: Pena-Burgos EM, Díez Corral MC, Ortiz-Cruz EJ, Bernabéu D, Tapia-Viñe M, A. Redondo, Pérez-Martínez A, Peláez A, Venegas Mascaró C, Escudero López A, and Pozo-Kreilinger JJ

Declaration of Conflicting Interests

The authors declared no potential conflicts of interest with respect to the research, authorship, and/or publication of this article.

Ethical Approval

Not applicable, because this article does not contain any studies with human or animal subjects.

Funding

The authors received no financial support for the research, authorship, and/or publication of this article.

Informed Consent

Consent for publication was obtained from the patient and/or families.

ORCID iD

Eva M. Pena-Burgos https://orcid.org/0000-0001-7113-045X

Trial Registration

Not applicable, because this article does not contain any clinical trials.

References

1. de Álava E, Lessnik S, Stamenkovic I. Ewing sarcoma. In: *WHO Classification of tumours of soft tissue and bone*. 5th ed. IARC Press; 2022:323-325.
2. Bator SM, Bauer TW, Marks KE, Norris DG. Periosteal Ewing's sarcoma. *Cancer*. 1986;58(8):1781-1784. doi:10.1002/1097-0142(19861015)58:8<1781::aid-cncr2820580835>3.0.co;2-h
3. Kolár J, Zídková H, Matějovsky Z, Povýsil C, Kolín J, Beran J. Periosteal Ewing's sarcoma. *ROFO Fortschr Geb Rontgenstr Nuklearmed*. 1989;150(2):179-182.
4. Wuisman P, Roessner A, Blasius S, Erlemann R, Winkelmann W, Ritter J. (Sub)periosteal Ewing's sarcoma of bone. *J Cancer Res Clin Oncol*. 1992;118(1):72-74. doi:10.1007/BF01192315
5. Shapeero LG, Vanel D, Sundaram M, et al. Periosteal Ewing sarcoma. *Radiology*. 1994;191(3):825-831. doi:10.1148/radiology.191.3.8184073
6. Declerck S, Devos V, Pattyn G. Periosteal Ewing sarcoma. *J Belge Radiol*. 1995;78(4):227.
7. Kollender Y, Shabat S, Nirkin A, et al. Periosteal Ewing's sarcoma: report of two new cases and review of the literature. *Sarcoma*. 1999;3(2):85-88. doi:10.1080/13577149977695
8. Hatori M, Okada K, Nishida J, Kokubun S. Periosteal Ewing's sarcoma: radiological imaging and histological features. *Arch Orthop Trauma Surg*. 2001;121(10):594-597. doi:10.1007/s004020100301
9. Delepine F, Delepine G, Cohen C, Delepine N. Periosteal Ewing's sarcoma. *Rev Chir Orthop Reparatrice Appar Mot*. 2002;88(2):188-192.
10. Erlemann R, Starker M. Juxtakortikaler tumor am distalen humerus. *Radiol*. 2002;42(2):125-129. doi:10.1007/s001170100629
11. Yoshida K, Kusuzaki K, Matsubara T, et al. Periosteal Ewing's sarcoma treated by photodynamic therapy with acridine orange. *Oncol Rep*. 2005;13(2):279-282.
12. Aymoré IL, Meohas W, Brito de Almeida AL, Proebstner D. Case report: periosteal Ewing's sarcoma: case report and literature review. *Clin Orthop*. 2005;434:265-272.
13. Hakozaki M, Hojo H, Tajino T, et al. Periosteal Ewing sarcoma family of tumors of the femur confirmed by molecular detection of EWS-FLI1 fusion gene transcripts: a case report and review of the literature. *J Pediatr Hematol Oncol*. 2007;29(8):561-565. doi:10.1097/MPH.0b013e3180f61ba3
14. Bonvin F, Merlini L. Periosteal Ewing sarcoma. *Pediatr Hematol Oncol*. 2007;24(5):369. doi:10.1080/08880010701252915
15. Bedard J, Burns J, de Comas A. Periosteal Ewing sarcoma in a 65-year-old man: a case report. *JBJS Case Connect*. 2017;7(2):e27. doi:10.2106/JBJS.CC.16.00168
16. Violon F, Burns R, Mihoubi F, et al. Intramedullary, periosteal, and extraskeletal Ewing sarcomas: retrospective study of a series of 126 cases in a reference center. *Skeletal Radiol*. 2022;51(8):1659-1670. doi:10.1007/s00256-021-03983-6
17. Kumar R, Mohanan S. Periosteal Ewing sarcoma: imaging features and clinical outcomes in 7 patients. *J Comput Assist Tomogr*. 2023;47(1):78-85. doi:10.1097/RCT.0000000000001382
18. Kenan S, Abdelwahab IF, Klein MJ, Hausman MR, Lewis MM. Case report 819: periosteal Ewing's sarcoma of the tibia. *Skeletal Radiol*. 1994;23(1):59-61. doi:10.1007/BF00203705
19. Maheshwari AV, Cheng EY. Ewing sarcoma family of tumors. *J Am Acad Orthop Surg*. 2010;18(2):94-107. doi:10.5435/00124635-201002000-00004